Available online at www.sciencedirect.com

SciVerse ScienceDirect

Procedia Engineering 58 (2013) 184 – 193

Procedia Engineering

www.elsevier.com/locate/procedia

The 12th Hypervelocity Impact Symposium

High Explosive Initiation Behavior by Shaped Charge Jet Impacts

Werner Arnold[a]*, Ernst Rottenkolber[b]

[a]*MBDA-TDW Gesellschaft für verteidigungstechnische Wirksysteme mbH, Hagenauer Forst, D-86529 Schrobenhausen, Germany*

[b]*NUMERICS GmbH, Mozartring 6, D-85238 Petershausen, Germany*

Abstract

In a recent study [5] the initiation behavior of Plastic Bonded High Explosives (PBX) when attacked by a Shaped Charge Jet (SCJ) was investigated. Two initiation modes: *Impact Initiation* and *Penetration Initiation* were distinguished by varying between *bare* and *covered test set-ups*, depending on the contact between the metal casing and the PBX. The transition between the two initiation modes was addressed by conducting more basic investigations with test setups allowing the study of these transition phenomena.

In the present work these more basic investigations were continued with theoretical studies on one hand supporting the findings in [5] by numerical simulations of the SCJ perforation and a simple analytic initiation model and on the other hand by additional trials applying lead as barrier material, increasing the sample diameter and splitting the sample charge into two parts.

Where possible the results were compared with older results from Held ([11] - [12]) achieved with TNT-bonded Comp B high explosive.

Selection and peer-review under responsibility of the Hypervelocity Impact Society

Keywords: Shaped Charge Jet, Impact / Bow Wave / Penetration Initiation Mode, Bare & Covered Charges, TNT-bonded & Plastic Bonded High Explosives, Numerical Simulation, Initiation Model.

1. Introduction

In a recent paper [5] the initiation behavior of a modern plastic bonded high explosive (PBX) KS32 (HMX/HTPB 85/15, ρ = 1.63 g/cc) and of a conventional TNT-bonded Comp B (RDX/TNT 65/35, ρ = 1.71 g/cc) when attacked by shaped charge jets (SCJ) was compared. Shaped charge jets usually have higher tip velocities (typically v_0 ~ 8 mm/µs) and smaller diameters (typically d ~ 3 mm) than standard projectiles. According to that the initiation behavior of high explosives when hit by a projectile can differ from that of SCJ impacts (see e.g. [1] and [2]). In [6] both impact situations were studied whereas in the present paper only SC jets will be considered. For Comp B a 44 mm caliber SC (SC-44) and for KS32 a 75 mm caliber SC (SC-75) was used. Two different initiation modes:

- Impact Initiation (prompt initiation, with very short run distances to detonation Δs ~ 10 mm)
- Penetration Initiation (initiation during penetration with run distances to detonation Δs >> 10 mm)

were distinguished while varying between *bare* and *covered test set-ups*, depending on the contact between the metal barrier P and the high explosive (Fig. 1). The standoff s/o between the SC and the steel barrier was 2 SC calibers. The run distance to detonation Δs was measured with a rotating mirror camera, while varying the SC jet stimulus v^2d (v = SCJ velocity, d = SCJ diameter). The comparison of the initiation results for both, KS32 and Comp B in *bare* and *covered setups* is shown in Figure 2 (taken from [5]). Both the enormous difference between the *impact (bare) initiation* vs. the *penetration (covered) initiation* mode and the transition behavior between these two modes were discussed intensively in [5]. Various possibilities

* Corresponding author. Tel.: *+49 (0) 8252-99-6267, Fax: +49 (0) 8252-99-6733*.
E-mail address: werner.arnold@mbda-systems.de.

Selection and peer-review under responsibility of the Hypervelocity Impact Society
doi:10.1016/j.proeng.2013.05.022

for the application of these findings on real (generic) munitions were addressed in several additional publications [6] – [8]. In the present paper, the study of these initiation modes will be further pursued by both supporting numerical simulation and applying an analytical model combined with additional fundamental experiments.

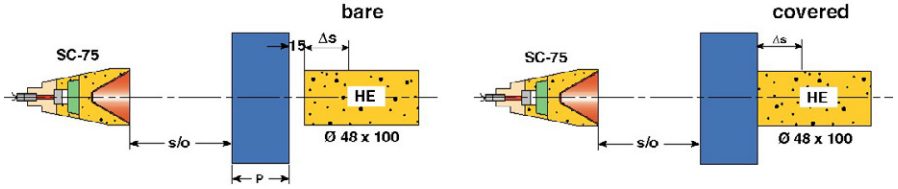

Fig. 1: Two different initiation test set-ups: bare (left) and covered (right).

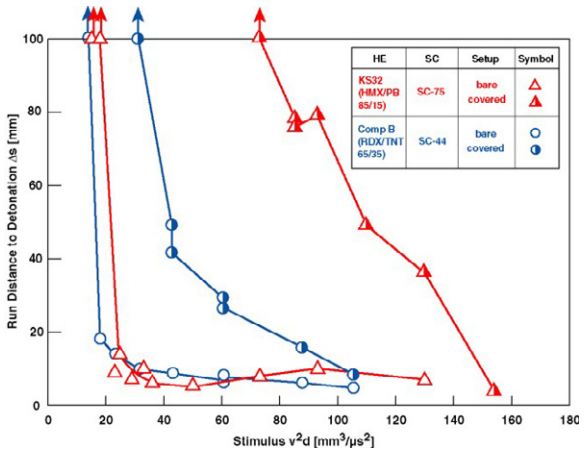

Fig. 2: Comparison of run distance to detonation Δs for bare and covered Comp B vs. KS32 when SCJ initiated with stimulus v^2d (v = SCJ velocity, d = SCJ diameter), (diagram taken from [5]).

2. Theoretical Considerations

The run distance to detonation Δs as reported in [5] was measured with a rotating mirror camera observing the outer free surface of the HE sample (the break through signal). But the very first initiation reactions occur more or less in the middle of the charge where the SC jet perforates it before the reaction front arrives at the surface of the charge. Thus, intrinsic features of the HE charge like corner turning distance, sensitivity etc. may influence the run distance results – this aspect should be taken into account. That is one reason why supplementary to [5] additional numerical simulations were conducted and also an analytical model was applied in a first step of this study. Another reason was to shed more light on the initiation behavior and thus to get a clearer understanding of what is happening when a SCJ perforates a HE sample. In a second step, additional basic tests were performed (see section 3).

Remark [3]: many observations and findings discussed in the following can be alternatively/additionally explained and interpreted with Backofen's "Kernel" model (see e.g. [4]).

2.1. Numerocal Simulations

The numerical simulations were conducted with the commercial hydrocode Autodyn. The SCJ was modeled as a stretching jet with an initial diameter of d_0 = 2.5 mm. The positions of the Lagrangian pressure gauges within the sample (diameter 48 mm, length 100 mm) are indicated in Figure 3 (the gauges at x = 20 mm depth are not shown here). The "HE-sample" was assumed as *inert*. Therefore, the simulated pressure curves are valid for a copper SCJ perforating equal density inert material. That means they are valid only for short penetration distances (say 10 – 20 mm) as afterwards chemical reactions may be initiated influencing the pressure profiles. Thus, the reliability of the profiles depends on the run distances to detonation.

2.1.1 Bare Charge

When a SCJ hits a bare HE sample, a shock wave with a very high pressure amplitude originates (Figs. 4 and 5 left). During the following penetration process, this pressure decreases rather rapidly. Usually the SCJ penetrates the sample supersonically and thus leads to a so called “bow wave” followed by a (ramp-like) pressure increase until the stagnation point is reached (Figs. 4 and 5 right). This very steep pressure increase causes the prompt initiation of the bare sample. Due to the “corner turning radius” it takes a Δs of about 10 – 20 mm until the detonation front appears at the outer free surface of the HE sample (Fig. 2). The v^2d amounts to about 25 $mm^3/\mu s^2$ for both bare Comp B and bare KS32. Due to the high strain rates the usually plastic behavior of the PB binder gets lost.

2.1.2 Covered Charge

When the steel barrier (to tune the SCJ energy = the v^2d stimuli) is in contact with the HE sample, completely different conditions prevail. With a 75 mm thick steel barrier, a bow wave is caused at 1 mm HE sample depth (Fig. 6 left) during the subsonic perforation of the steel plate. But due to the subsequent supersonic penetration in the HE sample, a second bow wave emerges which can be seen rather clearly at 20 mm sample depth (Fig. 6 right).

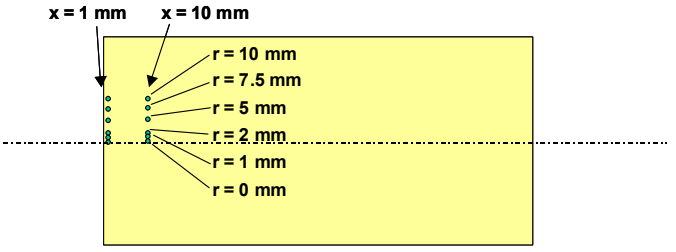

Fig. 3: Positions of pressure gauges within the HE sample (gauges at x = 20 mm depth are not indicated)

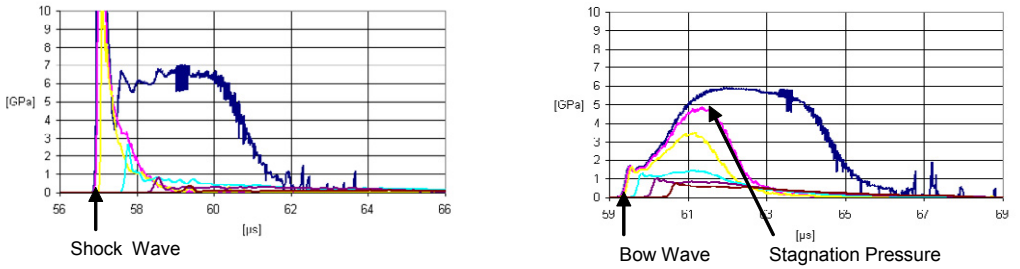

Fig. 4: High pressure shock wave at 1 mm depth (left). Evolving bow wave and stagnation pressure at 10 mm depth (right).

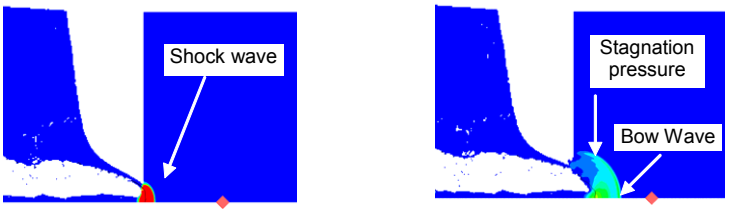

Fig. 5: Shock wave at 1 mm depth (left), bow wave and stagnation pressure at 10 mm depth (right).

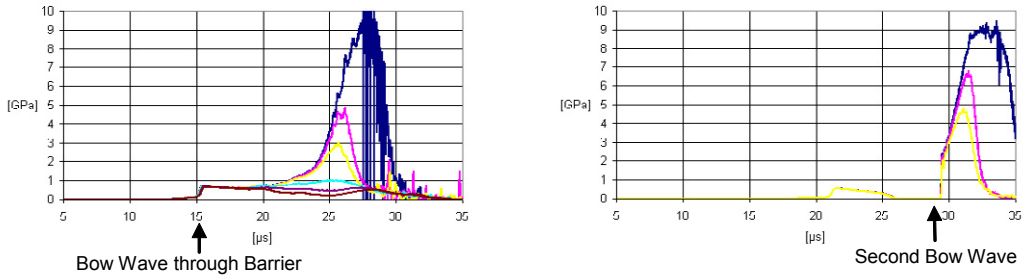

Fig. 6: Pressure profiles at 1 mm (left) and 20 mm depth (right) with 75 mm steel barrier in contact.

Comparing the experimental results taken from [5] between bare and covered setups in Figure 2 for KS32, we have to increase the v^2d stimulus (decrease the steel barrier thickness) from about 25 $mm^3/\mu s^2$ up to more than 70 $mm^3/\mu s^2$ (!) to get a detonation within the sample length of 100 mm. But now instead of a prompt initiation (*impact initiation mode*), the detonation starts at the very end of the sample (*penetration initiation mode*). While increasing the v^2d stimulus more and more, the run distance to detonation gets shorter and shorter until an almost prompt detonation is achieved within a very short run distance Δs at a $v^2d \sim 150$ $mm^3/\mu s^2$. This possibly means that a kind of SDT (shock-to-detonation transition) process takes place during the penetration of the SC jet where the run distance depends on the SCJ stimulus and we call that (in contrast to the prompt *impact initiation*) a *penetration initiation* mode – presumably comparable to the processes taking place in a gap test experiment.

As the detonation at the lowest stimulus always starts at the rear end of a HE sample (the same is true with cased charges, see [6] - [8]), the first bow wave (Fig. 6 left) is already attentuated and cannot be responsible for the initiation. Also phenomena like shock de-sensitization or closing of pores at the entrance side of the HE sample – these topics are sometimes discussed in the community - are irrelevant or play at the most a minor role in the initiation process. The *penetration initiation mode* process (SDT or nucleation-and-growth NAG) presumably starts somewhere between the second bow wave and the stagnation point (Figs. 5 & 6 right) with increasing reactions and rates while running along the axis until full detonation is achieved. Finally, the bright light breaking through signal on the sample surface is detected by the rotating mirror camera. Supporting simulations of emerging reaction processes with energetic material models were discussed in [9].

2.2. Analytical Model

A graphical description of a "virtual initiation point (VIP)" sketched by Held in [10] is shown in Figure 7. With Comp B he always measured a forward and rearward detonation front (see also section 3.2). Now, a simple analytical model shall be considered taking also the possibility of a radial extension of the VIP to a circular "initiation area" into account from which the detonation finally starts.

This new initiation model allows the possibility of an areal initiation and a subsequent spherical propagation of the detonation front sketched and parameterized in Figure 8 showing a cut through the sample (2-dimensional representative). Detonation is assumed to start at time t_0 at the outmost point (x_0, y_0).

The detonation propagates spherically with the velocity D and the distance to the initiation point is described by:

$$s(t) = D \cdot (t - t_0) \tag{1}$$

On the other hand, the geometrical relationship provides:

$$s(t) = \sqrt{(x - x_o)^2 + a^2} \tag{2}$$

Combining both relations:

$$t(x) = t_0 + \frac{1}{D}\sqrt{(x - x_0)^2 + a^2} \tag{3}$$

The parameters t_0, D, x_0 and a are used to fit the curves. Ideally they have the physical meaning:

- x_0: place where the first break through takes place (run distance to detonation Δs).
- D: Detonation velocity (for KS32 measured 8180 m/s).
- a: distance of the initiation point from the free surface of the HE sample. With an axial initiation a = 24 mm would be expected (sample diameter 48 mm).

The trial series presented in Figure 2 (see also [5]) were evaluated for KS32. Only the results for the parameter a will be discussed in the following (Fig. 9). There are two groups of results:

- With air gap (bare setup): a > 20 mm (with some scattering)
- Without air gap (covered setup): 5 mm < a < 20 mm dependent on steel barrier

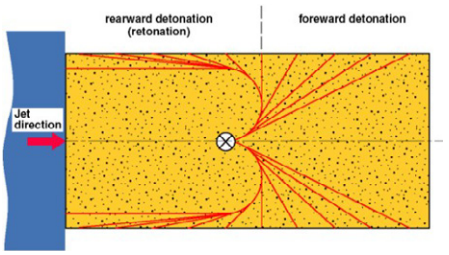

Fig. 7: Start of a detonation at the „virtual initiation point (VIP)“ with a forward and rearward detonation front [10].

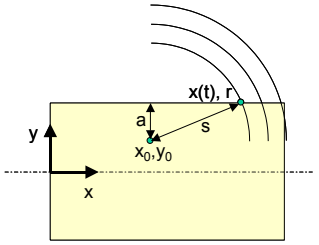

Fig. 8: Propagation of a spherical detonation wave starting from the edge of a virtual initiation plane with peripheral coordinate points (x_0, y_0).

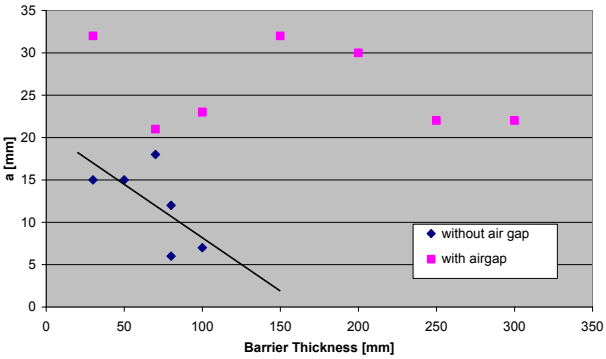

Fig. 9: Fitting parameter a vs. steel barrier thickness

2.2.1 Bare Charge

A prompt *impact initiation mode* is measured at run distances of $\Delta s \sim 0 - 20$ mm with necessary stimuli of $v^2d \sim 25\ mm^3/\mu s^2$ (see Fig. 2). An indicated virtual initiation area as sketched in Figure 10 (2-dimensional representative, left) by using for the parameters a ~ 20 mm and $\Delta s \sim 0 - 20$ mm.

2.2.2 Covered Charge

A trend can be perceived in Figure 9: a decreasing parameter "a" with increasing barrier thicknesses i.e. decreasing stimuli v^2d. For the two extreme situations: entrance and exit sides of the sample (see also Fig. 2):

- Entrance side: P ~ 20 mm, $v^2d \sim 140\ mm^3/\mu s^2$, a ~ 15 mm, $\Delta s \sim 0 - 20$ mm
- Exit side: P ~ 100 mm, $v^2d \sim 70\ mm^3/\mu s^2$, a ~ 5 mm, $\Delta s \sim 80 - 100$ mm

If these virtual initiation areas are drawn and interpolated in-between, then it results in a sketch as shown in Figure 10 (2-dimensional representative, right) for a *penetration initiation mode*. As described above, this supports an evolving SDT process as source for the initiation with increasing run distance to detonation with decreasing strength of the stimulus v^2d.

3. Experimental Tests

In the previous section 2 theoretical analyses were undertaken to further understand the results on SCJ initiation behavior achieved in [5]. In this section now, additional basic experimental tests shall be conducted to fill in the overall picture of the SC jet initiation behavior of a HE.

3.1. Bow Wave Initiation Model

In [5] either *impact initiation* or *penetration initiation* mode was measured. As shown in section 2.1.2, the pressure amplitude of the first bow wave caused in the steel barrier due to subsonic penetration is too small to cause an explosive initiation. This situation changes when replacing the barrier material steel with lead. Tests with Comp B were already reported by Held in [11]. In the present study his tests were repeated with KS32 experimentally and accompanied by numerical simulations.

Figure 11 shows the test setups with both a standard steel barrier and a lead barrier in contact with the HE sample. Held used the SC-44 shaped charge. Here the SC-75 shaped charge was applied. For each barrier material two different thicknesses were used:

- SC-44 (Comp B): Steel: $P_1 = 50$ and 75 mm; Lead: $P_2 = 42$ and 67 mm
- SC-75 (KS32): Steel: $P_1 = 50$ and 100 mm; Lead: $P_2 = 43$ and 87 mm

and adjusted in a way to get comparable SCJ stimuli v^2d. Accordingly, the standoffs s/o were chosen appropriately to be sure to have the same (particulated) jet parameters at the entrance of the HE. The HE sample size was the standard size with 48 mm diameter and 100 mm length and thus exactly the same as in [5] and [11]. The run distance to detonation Δs was again measured with a rotating mirror camera.

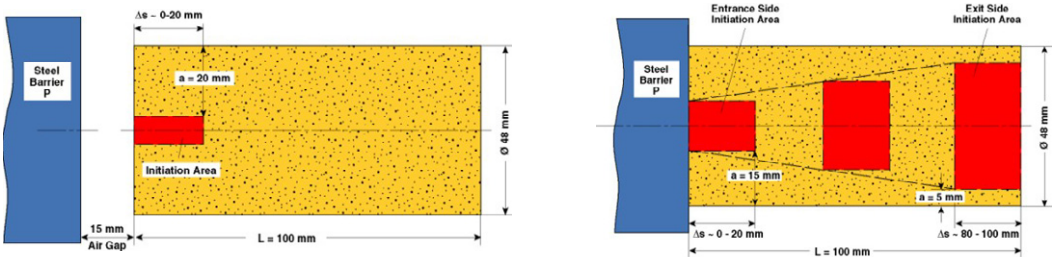

Fig. 10: Indicated virtual initiation areas for impact (bare setup, left) and penetration initiation mode (covered setup, right).

The results for Comp B and for KS32 are compared in Figure 12 showing the run distance to detonation Δs vs. the sum

of the standoff s/o and the barrier P. For both Comp B and for KS32, the run distance Δs is always much shorter with the lead barrier than with the appropriate steel barrier. Held suspected the different bulging effects due to the different ductility of the two materials to be responsible for this behavior. To check this assumption, additional numerical simulations were conducted.

Contrary to steel, lead has a very low sound velocity which leads to a relatively high and laterally extended bow shock wave. Figure 13 shows the different bow shock wave behavior (note the lateral extension) for lead (left) and steel (right) respectively after 16 µsec with the thinner barrier thicknesses. The bow wave for steel is not strong (and laterally extended) enough to initiate a prompt detonation but shows the typical penetration initiation mode with a relatively long run distance to detonation. After replacing it by lead, now the steep and laterally extended bow shock wave initiates both Comp B and KS32 more or less promptly, especially for high initiation stimuli (thinner barrier thicknesses). The run distances get larger with decreasing initiation stimuli (increasing barrier thicknesses).

The reason for this initiation behavior is not the bulging or the ductility effect, as suspected in [11] but the low sound velocity leading to a strong lateral extended bow wave. This means that in very special cases, additionally to the two known *impact initiation* and *penetration initiation* modes, a third mode emerges, the *bow wave initiation* mode.

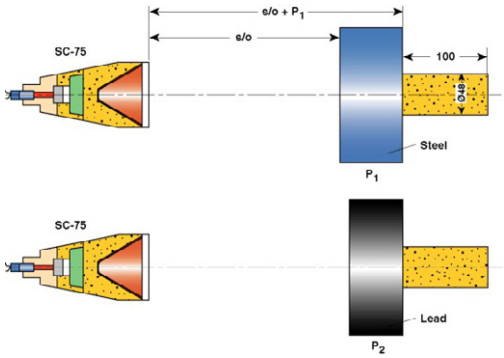

Fig. 11: Setups for the tests with steel and lead barriers respectively.

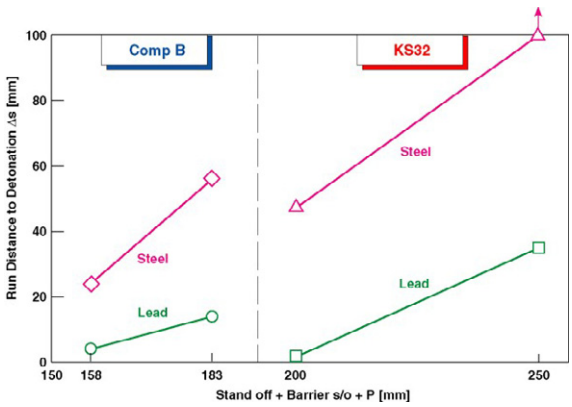

Fig. 12: Comparison of run distances for Comp B [11] and for KS32 when using steel or lead barriers respectively.

3.2. Larger Charge Diameter / Rearward Detonation

In section 2 a SDT process and a virtual initiation area were described as possible sources for the detonation front. It also

was mentioned that Comp B always showed in the streak mode pictures of the rotating mirror camera a forward and rearward running detonation front beginning from the break-through of the front (the break-through is the location, having the shortest distance between the initiation location and the charge surface). With KS32 only forward detonations were observed as Figure 14 shows exemplarily on the left (no rearward detonation). The ability of a detonation front to run around an inert obstacle (e.g. a corner: the "corner turning radius") is better for more sensitive high explosives as Comp B than for insensitive explosives like KS32.

These streak record observations are correlated with the analytical model, simulating the radial extension of the initiation source volume. If now the sample diameter is increased from the standard diameter 48 mm to 58 mm and the SCJ initiation test is repeated then both a forward and a rearward detonation (Figure 14 right) is observed - in consistency with the analytical model.

3.3. Split HE-Sample

This test series was also motivated by former tests from Held [12] with split HE test samples with Comp B. His reason to conduct this kind of test at that time was to study the influences of precursor shock waves, HE debris from the rear side of the first part of the test sample and things like that as well as to separate these from the real SCJ impact initiation. Some of his tests were repeated with KS32, but now with the background of distinguishing between *impact initiation* vs. *penetration initiation* mode (see also [8]). The KS32 standard sample with 48 mm diameter and 100 mm length was split into two 50 mm long parts with a 5 mm or 10 mm air gap in-between. In further tests, a 5 mm air gap was used and Held's 5 mm polyethylene disc was additionally introduced. As mentioned above, Held's motivation for the disc was to avoid any spall or debris cloud from the first HE part hitting the second charge. The steel barrier to tune the SC-75 shaped charge jet was 100 mm thick producing a stimulus of $v^2d = 73\ mm^3/\mu s^2$ not high enough to initiate a detonation in a covered test setup (Fig. 2).

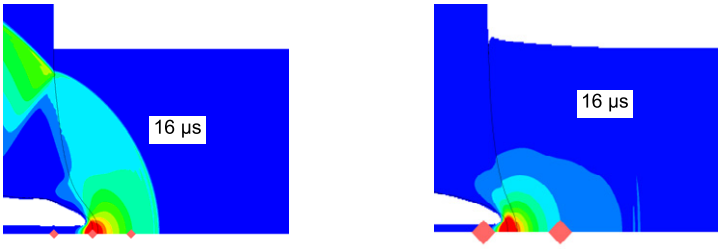

Fig. 13: Simulated bow shock wave pressure fields after 16 µsec for a lead barrier (left) and steel barrier (right) respectively. Color code: from dark blue p = 0 GPa to red p ≥ 10 GPa

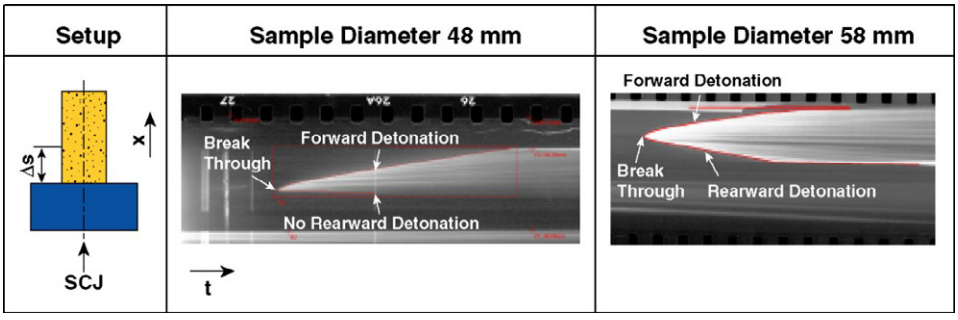

Fig. 14: Setup sketch with dashed line showing the streak slit for the camera (left). 48 mm sample diameter: streak record with only forward detonation (middle). 58 mm sample diameter: streak record with forward and rearward detonation (right).

The test results are summarized in Figure 15 indicated by the red triangles. The results are in good agreement with Held's findings in [12]. For all test variants a (prompt) initiation of the second KS32 part was observed (see the red triangles: forward detonation). Additional numerical simulations (not shown here) clearly confirmed the expected *impact*

initiation mode of a bare (or almost bare) charge due to the very high impact shock wave – and not due to debris. With KS32, the 5 mm polyethylene disc mitigates this impact shock not strongly enough to avoid an initiation (see also [5], [8]) – contrary to Comp B where no detonation occurred with the 5 mm polyethylene disc in contact to the "donor" charge (but also note: Held used the SC-44 resulting in a less "aggressive" impact shock wave).

Interestingly enough, the first part of the KS32 sample showed a rearward detonation (indicated by a reverse red triangle) despite the fact that the sample diameter is only 48 mm. That means either the detonation of the second part sympathetically initiates also the first part or possibly the sensitivity of this first part was increased by the perforation of the SCJ.

4. Conclusions

The theoretical considerations comprising numerical simulations as well as a simple analytical model supported the experimental findings in [5] concerning the two described SCJ initiation modes:

- Impact Initiation (prompt localized initiation, very short run distances to detonation $\Delta s \sim 10$ mm)
- Penetration Initiation (initiation during penetration, run distances to detonation $\Delta s >> 10$ mm)

when conducting the SCJ initiation experiments with *bare* or *covered* test setups respectively. The *impact initiation* mode is caused by very high and steep shock wave amplitudes entering the high explosive whereas the *penetration initiation* mode can be observed when a (steel) casing filters out this first shock wave. Now a SDT process (shock-to-detonation transition) takes place - comparable to the observations in a gap test experiment. These two different initiation modes were already intuitively exploited in [6] – [8].

In very special cases e.g. when exchanging the steel barrier material by a lead barrier material a third mode:

- Bow Wave Initiation (prompt lateral extended initiation, short run distances to detonation $\Delta s \sim 10$ mm)

can be observed. Due to the different material parameters of lead (very low sound velocity) compared to steel a relatively high and laterally extended *bow shock wave* emerges which is also able to initiate a prompt detonation. These basic experimental tests accompanying and completing the tests reported in [5] comprehensively confirm the initiation hypotheses proposed in [5] and in this work.

Acknowledgements

The authors would like to thank the BWB Team K 6.3 at Koblenz for funding this study.

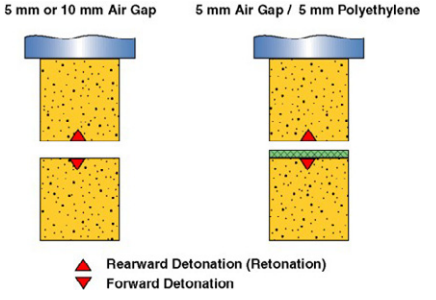

Fig. 15: Results with the split KS32 sample with 5 mm and 10 mm air gap, or 5 mm air gap and 5 mm polyethylene disc in contact with the second KS32 part showing in all cases a forward and rearward detonation.

References

[1] K.N. Lappo, S.N. Todd, M.U. Anderson, T.J. Vogler. *"Non-Shock Initiation of the Plastic Bonded Explosive PBXN-5: Experimental Results",* AIP Conference Proceedings, Shock Compression of Condensed Matter (SCCM) Waikoloa, Hawai'i, USA, June 24-29, 2007

[2] M.D. Cook, P.J. Haskins, R.I. Briggs, H. Flower, P. Ottley, A.D. Wood, P.J. Chheese . *"An Investigation into the Mechanisms Responsible for Delayed Detonations in Projectile Impact Experiments",* Proceedings of the 13th International Detonation Symposium, Norfolk, VA, USA, July 23-28, 2006

[3] J. E. Backofen. *Private communication, 2012*
[4] J. E. Backofen, *"Shaped charge jet initiation of explosives: a different view into penetration and initiation processes",* Proceedings of the 15th International Seminar New Trends in Research of Energetic Materials (NTREM), Pardubice, Czech Republic, April 18-20, 2012
[5] W. Arnold, E. Rottenkolber. *"Shaped Charge Jet Initiation Phenomena of Plastic Bonded High Explosives",* Proceedings of the 2012 Insensitive Munitions & Energetic Materials Technology Symposium (IMEMTS), Las Vegas, NV, USA, May 14-17, 2012
[6] W. Arnold. *"High Explosive Initiation by High Velocity Projectile Impact"* Proceedings of the 11th Hypervelocity Impact Symposium, Freiburg, Germany, April 11-15, 2010.
[7] W. Arnold, M. Graswald. *"Shaped Charge Jet Initiation of High Explosives equipped with an Explosive Train",* Proceedings of the 2010 Insensitive Munitions & Energetic Materials Technology Symposium (IMEMTS)
Munich, Germany, October 11-14, 2010.
[8] W. Arnold, E. Rottenkolber. "*Sensitivity of High Explosives against Shaped Charge Jets",* Proceedings of the 2007 Insensitive Munitions & Energetic Materials Technology Symposium (IMEMTS), Miami, FL, USA, October 15-18, 2007
[9] W. Lawrence, J. Starkenberg. *"The Effects of the Failure Diameter of an Explosive on its Response to Shaped Charge Jet Attack",* International Journal of Impact Engineering **20**, pp. 499-510, 1997
[10] M. Held. *"Diagnostic of Jet Initiation Phenomena",* Proceedings of the 25th Int. Congress on "High-Speed Photography & Photonics", SPIE 2002
[11] M. Held . *"Jet Initiation of Covered High Explosives with Different Materials",* Propellants, Explosives, Pyrotechnics **22**, 88-93, 2002
[12] M. Held . *"Shaped Charge Jet Initiation Tests with Covered High Explosive Charges with Air Gaps",* Propellants, Explosives, Pyrotechnics **26**, 38-42, 2001